

## The Profile of Mitochondrial Proteins and Their Phosphorylation Signaling Network in INS-1 $\beta$ Cells

Ziyou Cui,<sup>†,‡,§,#</sup> Junjie Hou,<sup>†,||,§</sup> Xiulan Chen,<sup>†,§,||,§</sup> Jing Li,<sup>†,||</sup> Zhensheng Xie,<sup>†</sup> Peng Xue,<sup>†</sup> Tanxi Cai,<sup>†,§</sup> Peng Wu,<sup>†</sup> Tao Xu,<sup>\*,†,§</sup> and Fuquan Yang<sup>\*,†,§</sup>

Laboratory of Proteomics, Institute of Biophysics, Chinese Academy of Sciences, Beijing 100101, China, Tianjin Key Laboratory for Biomarkers of Occupational and Environmental Hazard, Medical College of CAPF, Tianjin 300162, China, National Laboratory of Biomacromolecules, Institute of Biophysics, Chinese Academy of Sciences, Beijing 100101, China, and Graduate University of Chinese Academy of Sciences, Beijing 100049, China

Received November 03, 2009

Mitochondria have important roles in cellular physiological functions and various diseases. In pancreatic  $\beta$  cells, mitochondria play a central role in glucose-stimulated insulin secretion (GSIS). To reveal the potential functions of mitochondria in the GSIS process in  $\beta$  cells, shotgun proteomics was applied to profiling mitochondrial proteins and their potential phosphorylation sites in rat INS-1 cells. More than 800 proteins were assigned to mitochondria. In addition, 84 different mitochondrial phosphoproteins were identified, and 52 upstream kinases of mitochondrial phosphoproteins were predicted using bioinformatics tools. Regulation networks of mitochondrial phosphoproteins were constructed by integrating mitochondrial protein interaction networks and mitochondrial phosphorylation signaling, providing a preliminary survey of how phosphorylation signaling regulates mitochondrial function in  $\beta$  cells. We present integrated resources including the protein composition and signaling pathways of mitochondria which can be used to understand the role of mitochondria in GSIS.

**Keywords:** mitochondria •  $\beta$  cells • GSIS • proteome • mitochondrial protein phosphorylation • signaling network

### 1. Introduction

Mitochondria are highly dynamic and poly morphological organelles in mammalian cells. They are best known as the energy production plants of the cell. In addition, they play important roles in other cellular functions including fatty acid metabolism, apoptotic signaling, oxidative stress, ion homeostasis and biogenesis.<sup>1,2</sup> Because of their important roles in cellular physiology, defects in mitochondrial function may lead to a wide variety of diseases such as degenerative diseases, aging, cancer, myopathies, obesity, and diabetes.<sup>3</sup> Therefore, mitochondria have attracted a lot of research attention for the past several decades. To gain better insight into mitochondrial function, it is important to identify the complete set of mitochondrial proteins. With the rapid advance of proteomics, many proteomic methods have been applied to mitochondrial protein identification and characterization.<sup>1,4,5</sup> The first mitochondrial proteomic survey was carried out 10 years ago on human placental mitochondria using 2-DE followed by MALDI

analysis and led to the identification of 46 proteins.<sup>6</sup> Since then, large-scale proteomic investigations using shotgun or 1D PAGE coupled with LC-MS/MS methods have been performed on mitochondrial proteomes from different species, such as yeast,<sup>7–9</sup> humans,<sup>10,11</sup> mice,<sup>12,13</sup> and rats.<sup>14</sup> Pagliarini et al. performed an in-depth mitochondrial protein analysis of 14 mouse tissues and created a database of 1098 mitochondrial proteins.<sup>15</sup> This is the most complete mouse mitochondrial proteome at present. Although the size of the mammalian mitochondrial proteome was predicted by computational studies to be approximately 1500–2000 proteins, mitochondrial protein lists presented in previous studies contain far more than the true number of mitochondrial proteins.<sup>16,17</sup> In addition, different tissues and cells vary significantly in their mitochondrial functional requirements. As a result, the protein expression patterns of mitochondria differ in a tissue- and species-specific manner.<sup>16</sup> This has been demonstrated by several recent studies on the mitochondrial proteome from different tissues of mice and rats.<sup>12,14,15,18</sup> They found that about a half of all identified mitochondrial proteins were tissue-specific. Further analysis of tissue-specific and cell-specific mitochondrial proteins should shed further light on mitochondrial function.

However, clarifying the protein composition of mitochondria is a far cry from understanding mitochondrial function in detail. Accumulating evidence implies that reversible phosphorylation is involved in the regulation of mitochondrial function.<sup>19–22</sup> Several recent studies have focused on high-throughput iden-

\* To whom correspondence should be addressed. Prof. Fuquan Yang, e-mail, fqyang@ibp.ac.cn; tel. and fax, +86 10-64888581. Prof. Tao Xu, e-mail, xutao@ibp.ac.cn; tel., +86 10-64888436.

† Laboratory of Proteomics, Institute of Biophysics, Chinese Academy of Sciences.

‡ Tianjin Key Laboratory for Biomarkers of Occupational and Environmental Hazard.

§ National Laboratory of Biomacromolecules, Institute of Biophysics, Chinese Academy of Sciences.

# These authors contributed equally to this work.

|| Graduate University of Chinese Academy of Sciences.

tification of phosphorylation proteins in mitochondria by proteomic methods.<sup>23–28</sup> For instance, Lee et al. revealed 84 phosphorylation sites in 62 proteins in the mitochondrial fraction from mouse liver using IMAC coupled with MS/MS.<sup>25</sup> Reinders and colleagues used five independent experimental approaches and obtained 48 yeast mitochondrial proteins with a total of 80 phosphorylation sites.<sup>26</sup> These studies resulted in the first preliminary draft of the mitochondrial phosphoproteome. But these studies simply focused on the phosphoproteins identification; it remains unclear how these phosphorylated events are controlled by protein kinases and phosphatases, and to what extent these phosphorylated events carry out the elaborate regulation of mitochondrial function to meet the different needs of different tissues. To answer these questions, further studies to describe mitochondrial phosphoproteins and the specific effects of phosphorylation events in different tissues must be performed.<sup>22</sup>

As is well-known, mitochondria are pivotal in glucose-stimulated insulin secretion (GSIS) in pancreatic  $\beta$  cells. GSIS is triggered and elevated by metabolic coupling factors, or messengers derived from mitochondria.<sup>30–34</sup> It has been proposed that mitochondrial dysfunction is causally correlated with an insulin-secretion defect of  $\beta$  cells in diabetics.<sup>31–33,35</sup> Thus, comprehensive characterization of the  $\beta$  cell mitochondrial proteome is crucial for grasping mitochondrial function in-depth and further paving the way for understanding the mechanisms regulating GSIS in physiological and diabetic states. Here, for the first time, we have systematically profiled the protein composition and phosphoproteins of highly purified mitochondria from rat-derived INS-1  $\beta$  cells using shotgun proteomic methods to lay a foundation for determining the function of mitochondria during  $\beta$  cell insulin secretion. In this study, we identified about 850 mitochondrial proteins and 128 unique phosphopeptides in 84 different mitochondrial phosphoproteins. Protein interaction networks were constructed based on the mitochondrial proteins and phosphoproteins identified by bioinformatics methods. These interaction networks present an integrated overview of how mitochondrial proteins carry out various types of functions and how phosphorylation signaling regulates mitochondrial functions in  $\beta$  cells.

## 2. Materials and Methods

**2.1. Cell Culture.** INS-1 cells (China Center for Type Culture Collection, CCTCC) were cultured in RPMI 1640 medium containing 11 mM glucose, supplemented with 10% heat-inactivated FBS, 10 mM HEPES, 50  $\mu$ M 2-mercaptoethanol, 2 mM glutamine, 1 mM sodium pyruvate, 100 U/mL of penicillin, and 100 mg/mL of streptomycin, at 37 °C in a humidified atmosphere containing 5% CO<sub>2</sub>.

**2.2. Purification of Mitochondria.** Mitochondria were purified from INS-1  $\beta$  cells by Nycodenz density gradient centrifugation using the method of Okado-Matsumoto et al.<sup>36</sup> with slight modifications. INS-1 cells (5–6  $\times$  10<sup>8</sup>) were washed three times with ice-cold PBS (pH 7.4). Cells were then detached with a cell scraper (Corning) and suspended in 10 mL of ice-cold isolation buffer (250 mM sucrose, 2 mM HEPES, 1 mM EGTA, 0.1% BSA, pH 7.4, and protease and phosphatase inhibitors (Complete tablets and PhosSTOP, Roche, Mannheim, Germany). Cells were disrupted while on ice with a glass Dounce homogenizer (glass pestle and mortar) (Wheaton, Millville, NJ). Homogenization and all subsequent steps were performed at 4 °C. The homogenates were centrifuged at 800g for 10 min

(IEC MultiRF, Thermo Fisher Scientific, Waltham, MA). The resulting pellet was rehomogenized in 10 mL of isolation buffer and centrifuged at 800g for a further 10 min. The two supernatants were combined and centrifuged for 15 min at 20 000g. The resulting supernatant was collected as a soluble protein fraction (designated S) and frozen as aliquots at –80 °C for subsequent analysis. The pellet was washed with 5 mL of isolation buffer and centrifuged at 20 000g for a further 10 min. The resulting pellet (raw mitochondrial fraction) was resuspended in 5 mL of isolation buffer for Nycodenz gradient centrifugation. The resuspended mitochondrial fraction was combined with 5 mL of 50% Nycodenz dissolved in 5 mM Tris-HCl and 1 mM EDTA at pH 7.4 to give a 10 mL 25% Nycodenz/sample mixture. This Nycodenz/sample mixture was placed onto a 5 mL 40%, 5 mL 34%, 7 mL 30% discontinuous Nycodenz gradient and 7 mL 23% and 2 mL 20% Nycodenz were then placed on top of the sample mixture. The sealed tubes were centrifuged for 90 min at 52 000g at 4 °C. The mitochondrial fraction collected at the 25/30% interface was diluted 1:1 in ice-cold isolation buffer and centrifuged at 20 000g for 20 min to pellet the mitochondria. The purified mitochondrial pellet (designated M) was suspended in isolation buffer for subsequent analysis.

### 2.3. Evaluation of Mitochondrial Purity.

**2.3.1. Electron Microscope.** A mitochondrial pellet was fixed in 2.5% glutaraldehyde in isolation buffer at 4 °C for 2 h. After washing once in PBS buffer, the pellet was further fixed in 1% osmium tetroxide in PBS for 20 min at room temperature, dehydrated in a graded series of ethanol, and then carefully transferred to propylene oxide and embedded in Epon-Araldite. Ultrathin sections (50–70 nm thick) were cut on a Leica EM UC6 Ultramicrotome (Leica, Milton Keynes, U.K.) with a diamond knife, loaded onto Formvar-carbon coated copper grids, stained with saturated uranyl acetate followed by lead citrate, and then examined on an electron microscope at 120 kV.

**2.3.2. Western Blotting.** One dish of INS-1 cells was washed twice with ice-cold PBS and lysed in 8 M urea containing a protease inhibitor cocktail. After sonication, the cell lysate was centrifuged at 20 000g for 45 min and the supernatant (total cell lysate, TL) was collected. The supernatant collected during cellular fractionation in the mitochondrial isolation process (designated S) was precipitated with methanol/chloroform and solubilized in 8 M urea. Protein concentration of the three subcellular fractions (TL, S, and M) was then determined with the Bradford method. For Western blotting, equal amounts of subcellular fractions were separated by SDS-PAGE and electroblotted onto 0.45  $\mu$ m Hybond-P PVDF membranes (GE Healthcare, Piscataway, NJ). The membranes were probed with various primary and corresponding secondary antibodies against marker proteins from different cellular compartments. Immunoreactive proteins on the membranes were then detected using a SuperSignal West Femto kit and exposed to X-ray film. The grayscale of Western blotting was quantified using ImageQuant TL (GE Healthcare, Piscataway, NJ). Western blots were repeated three times for every selected protein from every batch of total subcellular fractions.

**2.3.3. Respiration Control Ratio.** The mitochondrion is the center of energy metabolism and one of the indices for evaluating the function of oxidative phosphorylation in mitochondria is the respiration control ratio (RCR). In the present research, mitochondrial respiratory function was measured with a Strathkelvin 1302 oxygen electrode attached to a Strathkelvin 928 multichannel dissolved oxygen meter (Strathkelvin Instruments, Glasgow). Briefly, purified mitochondrial

protein (500  $\mu\text{g}$ ) suspended in 200  $\mu\text{L}$  of isolation buffer was added to 1 mL of reaction buffer (225 mM mannitol, 70 mM sucrose, 1 mM EDTA, 0.1% BSA, 10 mM PBS, pH 7.4). After a stable baseline was obtained, 10  $\mu\text{L}$  of 0.2 M disodium succinate was added to the reaction system as a substrate to a final concentration of 5 mM. This initiated "state IV" respiration. After recording for 3 min, 4  $\mu\text{L}$  of 50 mM ADP was added to initiate "state III" respiration and the reaction curve was recorded for another 10 min. The respiration control ratio was calculated according to the recorded curves using the software provided (Strathkelvin 928 data analysis module, version 2.3.1.12).

**2.4. In-Solution Digestion with Trypsin.** In-solution digestion of mitochondrial proteins was carried out using an optimized MS-compatible surfactant and organic solvent method. In this research, mitochondrial proteins suspended in isolation buffer were precipitated with methanol/chloroform. The pellet was solubilized by adding 20  $\mu\text{L}$  of 5 $\times$  invitrosol LC/MS surfactant, blended and incubated at 60 °C for 5 min. Then, 80  $\mu\text{L}$  of 80% acetonitrile (ACN), 20% 100 mM NH<sub>4</sub>HCO<sub>3</sub> was then added to the sample. This sample mixture was sonicated for 2 h. The sample was then reduced with 10 mM DTT for 1 h at 56 °C, and alkylated with 40 mM iodoacetamide in the dark for 45 min at room temperature before adding 40 mM DTT to quench the iodoacetamide and incubating for a further 30 min at room temperature. Sequence grade trypsin was then added at an enzyme/protein ratio of 1:30 and digested at 37 °C overnight. Tryptic digestion was stopped by adding formic acid (FA) to a final concentration of 1%. The peptide mixture was analyzed by LC-MS/MS or was used to enrich phosphopeptides.

**2.5. Enrichment of Phosphopeptides with IMAC and TiO<sub>2</sub>.** Self-packed C<sub>18</sub> columns were prepared by packing 50 mg of C<sub>18</sub> material (40–60  $\mu\text{m}$ , 120-Å pore size, SunChrom, Deutsche) into 1.5 mL AGT Cleanert SPE columns (about 0.3 mL bed volume) for sample desalting. Prior to enrichment of phosphopeptides, the peptide mixture (2 mL) of 2 mg of mitochondrial proteins was loaded on the C<sub>18</sub> column. The column was then washed five times with 1.0 mL of 0.1% TFA, and was eluted with a series of elution buffers (1.0 mL) containing 0.1% TFA/X% ACN, in which the percentage of ACN (X) was either 10%, 15%, 20%, 25%, 30%, 35%, 40%, 50% or 100%. All fractionates were combined, dried with a Speed-Vac and stored at –20 °C for further use. The desalted sample was divided into two shares for phosphopeptide enrichment using Fe<sup>3+</sup>-IMAC and TiO<sub>2</sub>. The IMAC column was packed with POROS 20 MC particles (Applied Biosystems) in a 1.5 mL AGT Cleanert SPE column (0.3 mL bed volume). The Fe<sup>3+</sup> IMAC procedure included the following steps: the IMAC column was first washed separately with 5 $\times$  column volumes (CV) of 100 mM EDTA and deionized water. Fe<sup>3+</sup> ion was then loaded onto the resin of the column with 5 CV of 100 mM FeCl<sub>3</sub> (in 100 mM acetic acid). After washing with 5 CV of 100 mM acetic acid to remove superfluous Fe<sup>3+</sup>, half of the desalted sample was dissolved in 100 mM acetic acid and loaded onto the IMAC column. The flow-through fraction was loaded onto the column again for maximum binding. To remove nonspecific bound peptides, the column was washed with 5 CV of 100 mM NaCl (in ACN/H<sub>2</sub>O/acetic acid, 24/75/1, v/v/v). Finally, phosphopeptides were eluted from the column with 0.3 M ammonia (NH<sub>3</sub>·H<sub>2</sub>O) in 5% ACN. The elution fraction was dried in a speed vacuum, and reconstituted in 0.1% FA for LC-MS/MS analysis. Enrichment of phosphopeptides with TiO<sub>2</sub> was performed according to the method of Wu et al.<sup>37</sup> The remaining

desalted sample was dissolved in binding solution (2% TFA/65% ACN solution saturated with glutamic acid) and added to a 1:1 slurry of TiO<sub>2</sub> beads (in binding solution). Peptides and TiO<sub>2</sub> beads were agitated at room temperature for 1 h, and then washed separately with binding solution, 0.5% TFA/65% ACN and 0.1% TFA/65% ACN. Bound peptides were eluted twice with 0.3 M ammonium hydroxide in 50% ACN, and finally acidified with 1% FA. The fractions were pooled and dried in a Speedvac, and dissolved in 0.1% FA for analysis by mass spectrometry.

**2.6. 2D-nanoLC-MS/MS Analysis.** The digested mitochondrial peptide mixtures were centrifuged at 13 000g for 10 min and the pellet was discarded prior to analysis. The supernatant was analyzed using a high-throughput tandem mass spectrometer LTQ ion trap (Thermo Fisher Scientific, Waltham, MA) equipped with an in-house built nanoelectrospray device.<sup>38</sup> The HPLC system used was equipped with a Surveyor pump (Thermo Fisher Scientific, Waltham, MA). For single analyses, 100  $\mu\text{g}$  of peptide mixtures was pressure-loaded onto a two-dimensional capillary column (250  $\mu\text{m}$  i.d.) packed with 3 cm of a C<sub>18</sub> resin (Sunchrom 5  $\mu\text{m}$ , Germany) and 3 cm of a strong cation exchange resin (Luna 5  $\mu\text{m}$  SCX 100A, Phenomenex). The buffer solutions used were 5% ACN/0.1% FA (buffer A), 80% ACN/0.1% FA (buffer B), and 500 mM ammonium acetate/5% ACN/0.1% FA (buffer C). The two-dimensional column was first desalted with buffer A and then eluted using a 12-step salt gradient ranging from 0 to 500 mM ammonium acetate. The effluent peptides from the two-phase column from each step were directed onto a 10 cm C<sub>18</sub> analytical column (100  $\mu\text{m}$  i.d.) using a 3–5  $\mu\text{m}$  spray tip. Step 1 consisted of a 80-min gradient from 0% to 100% buffer B. Steps 2–12 had the following profile: 3 min of 100% buffer A, 5 min of X% buffer C, a 5-min gradient from 0% to 10% buffer B, a 77-min gradient from 10% to 45% buffer B, a 10-min gradient from 45% to 100% buffer B, and a final 10 min of 100% buffer B. The 5-min buffer C percentages (X) were 5%, 10%, 15%, 20%, 25%, 30%, 40%, 50%, 60%, 80% and 100%, respectively. Nanoelectrospray ionization was accomplished with a spray voltage of 2.2 kV and a heated capillary temperature of 200 °C. A cycle of one full-scan mass spectrum (400–2000  $m/z$ ) followed by five data-dependent tandem mass spectra was repeated for each step of the multidimensional separation. All tandem mass spectra were collected using normalized collision energy (a setting of 35%), an isolation window of 3  $m/z$ , and 1 microscan. The application of mass spectrometer scan functions and HPLC solvent gradients were controlled by the XCalibur data system (Thermo Fisher, Waltham, MA).

**2.7. Analysis of MS/MS Data.** The SEQUEST algorithm (licensed to Thermo Finnigan) was used to search the MS/MS raw spectra against the target-decoy rat Refseq Database (version 2007.03.18, National Center for Biotechnology Information). The database search was performed using the following parameters for peptide identification: two missed cleavage sites were allowed, a fixed modification of 57.02 on cysteines, a variable modification of 15.99 on methionines, a mass tolerance of 2.0 Da for peptides (average mass) and 1.0 Da for fragment ions (monoisotopic mass). The searched results were analyzed in batches using TPP GUI (Trans-Proteomic Pipeline, V3.5, <http://tools.proteomecenter.org/software.php>). The resulting INTERACT XML files were merged and analyzed by ProteinProphet for statistical evaluation of protein identifications.<sup>39,40</sup> A ProteinProphet probability score of  $\geq 0.9$  was used. Furthermore, proteins identified by a single peptide with an

identification probability of  $<0.9$  were also excluded in this study. To create a nonredundant database, protein identifications were examined manually for possible redundancies. The search parameters used for identification of phosphorylated proteins, in addition to the search parameters used for total protein identification mentioned above, included a differential modification of 79.966 on serines, threonines, and tyrosines. Phosphorylation sites were analyzed by first filtering the search results with parameters including  $Rsp \leq 1$  and  $\Delta Cn \geq 0.1$ . Second, all peptide matches were filtered by XCorr (XCorr thresholds were set as 1.5, 2.0, and 2.5 for singly, doubly, and triply charged ions, respectively) and then all the initial filtered phosphopeptide spectra were manually validated with the aid of DTASelect's GUI, which is a subfunction of DATSelect for displaying the MS spectra of peptides.<sup>41</sup> Finally, these filtered phosphopeptides were analyzed using the Ascore algorithm, a probabilistic algorithm that predicts the likelihood of matching site-determining ions to specific phosphorylation site locations.<sup>42</sup> Only phosphorylation sites with an Ascore  $\geq 19$  ( $p < 0.01$ ) were considered accurately assigned.

**2.8. Data Mining and Bioinformatics.** The subcellular locations of identified proteins were annotated using the GO database and Swiss-Prot/TrEMBL protein knowledgebase. Subcellular locations of proteins were predicted with TargetP 1.1<sup>43</sup> (<http://www.cbs.dtu.dk/services/TargetP/>), Mitoprot<sup>44</sup> (<http://ihg2.helmholtz-muenchen.de/ihg/mitoprot.html>), Predator<sup>45</sup> (<http://urgi.versailles.inra.fr/predotar/predotar.html>) and SubLoc<sup>46</sup> (<http://www.bioinfo.tsinghua.edu.cn/SubLoc/>). Proteins with GO database or Swiss-Prot/TrEMBL protein knowledgebase mitochondrial location annotations were accepted as mitochondrial proteins. Proteins without mitochondrial annotations which were predicted by at least two of the above-mentioned programs to be, or possibly be, located in mitochondria were also accepted as mitochondrial proteins. In addition, we compared our results with previous literature on the rat mitochondrial proteome to retrieve mitochondrial proteins missed by the above two methods (literature curation). Finally, redundant proteins were removed by manual checking.

The transmembrane domains of the mitochondrial proteins identified were predicted in batches with TMHMM 2.0 (<http://www.cbs.dtu.dk/services/TMHMM/>). Molecular weights, theoretical pI values, and GRAVY index scores were predicted with ProtParam (<http://cn.expasy.org/tools/protparam.html>).<sup>47</sup> Codon Adaptation Indexes (CAIs) were predicted in batches by CodonW (<http://mobyle.pasteur.fr/cgi-bin/MobylePortal/portal.py?form=codonw>). The functional categorization of identified proteins was carried out using the PANTHER classification system ([www.pantherdb.org](http://www.pantherdb.org)).<sup>48,49</sup> They were then mapped to rat metabolic pathways in the Kyoto Encyclopedia of Genes and Genomes (KEGG) database using their rat NCBI gene IDs. The protein interaction prediction system STRING 8.0 (<http://string.embl.de/>) was used to retrieve protein associations.<sup>50</sup> The gene names of all mitochondrial proteins identified were input into the STRING system to retrieve the protein interactions. NetworKIN-2.0 was used to predict kinase–substrate relationships by submitting the protein sequences and corresponding phosphorylation sites of all the phosphoproteins. The human database was used since it has greater homology to *Rattus norvegicus* than other optional species.<sup>51</sup> Finally, a network diagram of mitochondrial phosphoprotein associated interactions was generated using Cytoscape (Version 2.4.1).<sup>52</sup>

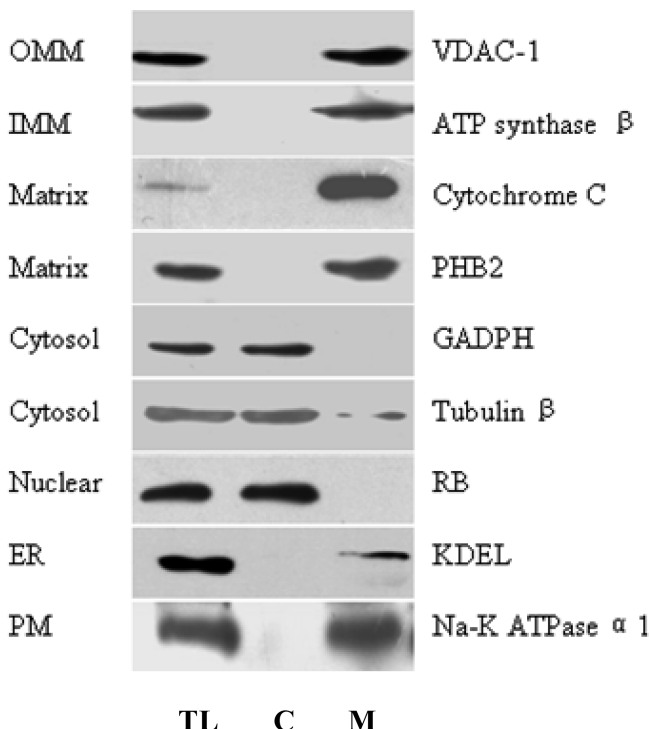


**Figure 1.** Verification of the purity of isolated mitochondria by Western blotting. Western blotting was performed on total cell lysis (TL), cytosol (C), and mitochondrial (M) fractions after cellular fractionation. IMM, inner mitochondrial membrane; OMM, outer mitochondrial membrane; Matrix, mitochondrial matrix.

### 3. Results and Discussion

**3.1. The Purity and Integrity of Isolated INS-1 Mitochondria.** High mitochondrial purity is a primary prerequisite for accurate determination of the mitochondrial proteome. Highly pure preparations of mitochondria will exclude contamination from other suborganelles and minimize false-positive identification of mitochondrial proteins. In our study, a loose-fitting Dounce homogenizer was used to homogenize INS-1  $\beta$  cells to reduce the number of broken mitochondria. Subsequently, mitochondria were purified by Nycodenz density gradient centrifugation following differential centrifugation.<sup>36</sup> To evaluate the quality of the mitochondria isolated, EM, Western blotting, and measurement of the respiration control ratio (oxygen consumption) were used to assess the morphology, purity, and functional integrity of the isolated mitochondria, respectively. First, the ultrastructure of purified mitochondria was examined by EM (SI Figure 1). Most mitochondria were intact, and both outer and inner membrane ridges could be seen. Second, several subcellular markers, including mitochondrial proteins (ATP synthase  $\beta$ , cytochrome c, PHB2, and VDAC-1), cytosol proteins (GADPH, and tubulin- $\beta$ ), a plasma membrane (PM) protein (Na-K ATPase  $\alpha 1$ ), an endoplasmic reticulum (ER) protein (KDEL), and a nuclear protein (RB) were detected by Western blotting (Figure 1). While cytosol and nuclear proteins were effectively removed after several fractionating steps, the PM protein Na-K ATPase  $\alpha 1$  and the ER protein KDEL still remained in the mitochondrial fraction. Proteins located in every part of the mitochondria, including the inner membrane, the outer membrane, and the matrix of the mitochondria, were readily detected, indicating that whole mitochondria were greatly enriched. Finally, oxygen consump-

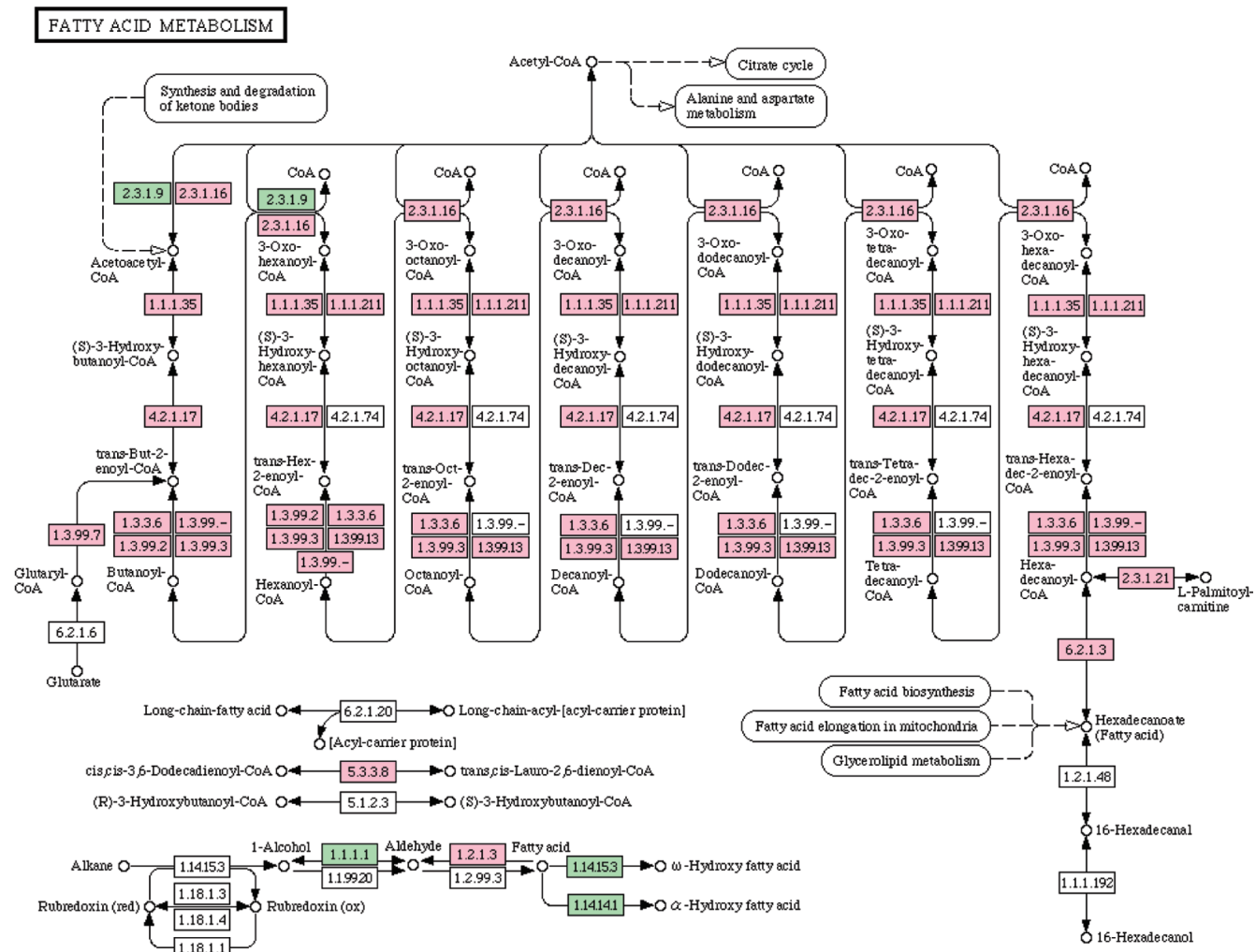
tion was checked with an oxygen electrode to estimate the integrity of the isolated mitochondria.<sup>53</sup> When succinate was added to the mitochondrial suspension, basal activity of the respiratory chain shifted rapidly to state-3 respiration. State-3 respiration then switched quickly to state-4 respiration on addition of ADP (SI Figure 2), indicating that the respiratory chain worked well in the isolated mitochondria, that is, that most mitochondria in the last fraction remained intact. From these results, it can be seen that intact mitochondria were greatly enriched in our study. However, isolation of highly pure mitochondria is very challenging because mitochondria have close contact with an extensive network of other membrane-bound compartments and are closely intertwined with the cytoskeleton and its associated proteins. In this study, although intact mitochondria were well fractionated, protein contaminants, especially from the ER and PM, could not be completely excluded from the samples.

**3.2. Profile of the Rat  $\beta$  Cell Mitochondrial Proteome.** Mitochondria are double-membraned compartments with many hydrophobic membrane proteins. To get as many peptides as possible from these hydrophobic proteins, the MS-compatible surfactant invitrosol and the organic solvent ACN were used together to promote protein dissolution and digestion.<sup>54</sup> After in-solution digestion, peptides were subjected to 2D-nanoLC-MS/MS analysis. Using target-decoy rat Refseq Database searching, 1917 proteins were identified with protein possibility scores  $\geq 0.9$  using the TPP platform,<sup>39,40</sup> which ensured a false positive rate (FPR) below 1% (SI Table 1). To annotate the subcellular locations of the proteins, these identified proteins were mapped with the GO database, the Swiss-Prot/TrEMBL protein knowledgebase and the Panther gene annotation system, and 510 proteins were annotated to be located in the mitochondria. The rest of the proteins were then submitted to four online programs, TargetP, Predator, MitoProt II, and SubLoc, to predict their subcellular locations. The former three programs are designed for systematic screening of the subcellular locations of proteins by recognizing the N-terminal targeting sequences. SubLoc identifies protein subcellular location according to amino acid composition. Proteins predicted as mitochondrial proteins by TargetP must have a specificity cutoff value  $>0.95$ , and those predicted by MitoProt II have a cutoff value  $>0.5$ . Default parameters were used in the other two prediction programs. To minimize false positive mitochondrial protein prediction, only proteins predicted by at least two programs to be located or possibly located in mitochondria were accepted as mitochondrial proteins. According to this criterion, another 267 proteins were predicted to be located in the mitochondria. An additional 51 of the proteins identified here were reported to be mitochondrial proteins in Forner's work on the rat mitochondrial proteome.<sup>14</sup> Forner et al. used a combination of Mitopred, PSORT and protein correlation profiling to identify of proteins residing in the mitochondria.<sup>14</sup> On the basis of the aforementioned methods, 828 proteins were included in the final list of the rat INS-1  $\beta$  cell mitochondrial proteins (SI Table 2).

After protein identification, the physiochemical characteristics of mitochondrial proteins identified in our study, including their pI values, MWs, GRAVY values, transmembrane domains, and CAI values, were computed by several Web-based programs (SI Figure 3). The pI values of identified mitochondrial proteins were between 4 and 12 (SI Figure 3A), with most clustering around 6.0–6.5, 6.5–7.0, and 8.0–10.0. More than half (61%) of the identified mitochondrial proteins had pI values

of  $\geq 8.0$ , in line with the results of Taylor<sup>10</sup> and Zhang.<sup>13</sup> The MW of mitochondrial proteins ranged from 10–60 kDa (SI Figure 3B). To demonstrate the hydrophobic properties of the identified mitochondrial proteins, GRAVY values and transmembrane domains were estimated (SI Figure 3C,D). Proteins with CAI values of 0–0.1 were the most prevalent mitochondrial proteins present in our study (SI Figure 3E), indicating that most mitochondrial proteins might be expressed at very low abundance. The above analysis has shown that most mitochondrial proteins are alkaline with low molecular weight and low abundance.

**3.3. Functional Classification and Functional Interactions of the Identified Mitochondrial Proteins.** To obtain a general functional overview of the mitochondrial proteins identified here, protein classification, metabolic protein pathway, and protein–protein interactions were analyzed using PANTHER,<sup>48,49</sup> KEGG,<sup>55</sup> and STRING,<sup>50</sup> respectively. All protein identity numbers were input into PANTHER and a total of 816 genes were matched to 30 functional groups (SI Table 2). The gene names of all identified mitochondrial proteins were then input into STRING to retrieve the protein interactions. A total of 730 gene names were mapped to the database of mouse protein interactions, and 3345 pairs of interacting proteins involving 438 proteins were obtained (SI Figure 4). The figure shows protein–protein interactions (PPIs) that form functional clusters in mitochondria. The density of these PPIs also indirectly indicates that these proteins interact with known mitochondrial proteins that are possibly located in the mitochondria. KEGG pathway analysis matched 270 proteins to 76 metabolic pathways (SI Table 3), of which 64 proteins mapped to oxidative phosphorylation (29 separate polypeptide chains of NADH dehydrogenase (Complex I), 4 subunits of succinate dehydrogenase (Complex II), 6 protein subunits of cytochrome c reductase complex (Complex III), 8 subunits of cytochrome c oxidase (Complex IV) and 13 subunits of F-type ATPase (Complex V)) (SI Figure 4). These proteins interact tightly with other function-associated proteins as shown in SI Figure 4. In addition, 25 proteins were mapped to the fatty acid metabolism pathway (Figure 2). Since fatty acid metabolism is critical for insulin secretion,<sup>56</sup> alteration of these key enzymes of fatty acid metabolism or the disturbance of fatty acid metabolism can impair insulin secretion. Herrero et al. found that overexpression of LCPTI could alter insulin secretion through increasing malonyl-CoA.<sup>57</sup> Using KEGG analysis, 18 carbohydrate metabolism-related proteins were matched to the TCA cycle; other proteins were identified as the rate-limiting enzymes of the TCA cycle (SI Figure 6). It is known that the metabolism of glucose via the TCA cycle provides many intermediates for the regulation of insulin secretion in  $\beta$  cells.<sup>34</sup> The detection of this protein class is helpful for further deciphering the roles of the carbohydrate metabolic pathway in  $\beta$  cell insulin secretion. On the basis of the above analysis, individual mitochondrial proteins identified were integrated into functional networks, and these mitochondrial proteins were grouped into the following main functional families: metabolism, electron transport, transport, intracellular protein trafficking, protein targeting and localization, immunity and defense, signal transduction, apoptosis, homeostasis, developmental processes, cell structure and motility, cell cycle, cell proliferation and differentiation (Table 1). The potential functions of every protein



00071 7/11/08

**Figure 2.** The identified components of fatty acid metabolism presented in KEGG pathway. Protein names highlighted in red are proteins identified in this study.

**Table 1.** The classification of mitochondrial proteins identified in this study

category name	gene hit
Metabolism	538
Biological process unclassified	175
Electron transport	89
Transport	83
Intracellular protein traffic	49
Immunity and defense	30
Signal transduction	26
Developmental processes	21
Cell structure and motility	17
Apoptosis	16
Cell cycle	13
Cell proliferation and differentiation	11
Protein targeting and localization	10
Oncogenesis	8
Homeostasis	5
Other functions	16

group of the more important mitochondrial proteins in INS-1  $\beta$  cells were analyzed further (SI Data 1).

**3.4. Mitochondrial Phosphoproteins and Their Phosphorylation Sites Identified in INS-1  $\beta$  Cells.** To further explore the possible functions of the mitochondrial proteins identified,

mitochondrial phosphoproteomic analysis was performed using multidimensional protein identification technology (Mud-PIT). Using highly purified mitochondria, phosphorylated peptides were enriched using  $\text{Fe}^{3+}$ -IMAC/TiO<sub>2</sub> following in-solution digestion with trypsin, and analyzed by 2D-nano LC-MS/MS. Using the filtering parameters mentioned in the Materials and Methods and manual validation of phosphopeptide spectra, 84 mitochondrial proteins were detected with 128 unique phosphopeptides (SI Data 2 and SI Table 4). The Ascore value was calculated to determine the precision of phosphorylation site,<sup>42</sup> and only the sites with an Ascore  $\geq 19$  ( $P < 0.01$ ) were considered confidently assigned. To further verify the identified phosphopeptides, the eight peptides with known or novel phosphorylation sites were synthesized (Beijing Scilight Biotechnology Ltd. Co. Beijing, China), and analyzed using MS/MS. As shown in Figure 3, it was clear that very high similarity of a pair of MS/MS spectra between identified (A) and synthetic (B) phosphopeptides indicated high accuracy of identified phosphorylation site. Other results of verification were shown in SI Data 3. Compared with previous studies, we identified not only many previously reported phosphoproteins, such as PDHA1, the 18 kDa protein, HSP90, VDAC, AKAP1, CYB5R3, TOMM 70 A, and CKMD1, but also some new

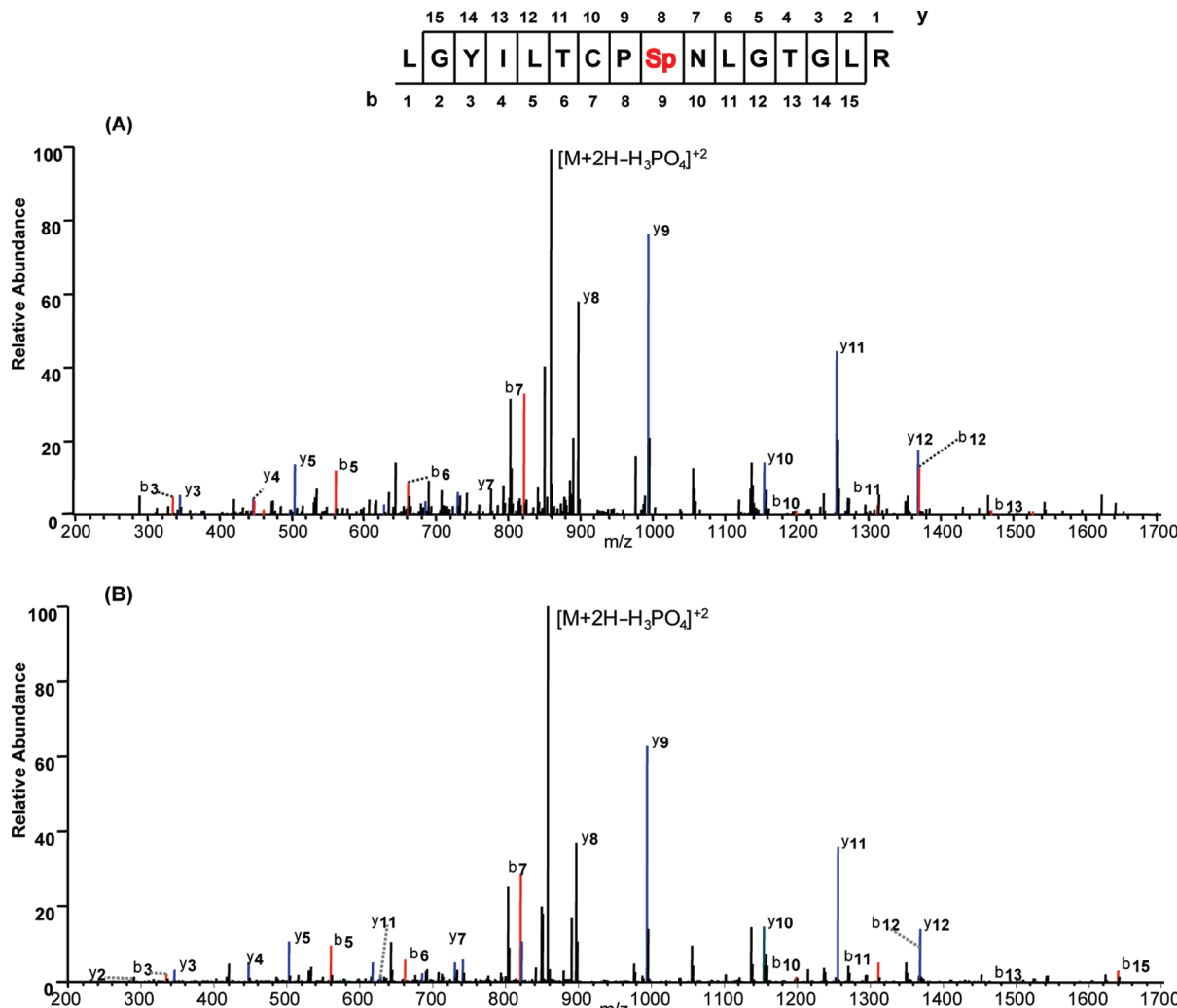


**Figure 3.** Experimental verification of phosphorylated peptides by MS/MS of synthetic peptides. The tandem mass spectra between synthetic and identified phosphopeptides show similar ion series and intensity. (A) The spectrum of identified phosphorylated peptides LGYILTCPSpNLGTGLR from ubiquitous mitochondrial creatine kinase from the mitochondrial extract of INS-1 cells. (B) The spectrum of the synthetic peptide corresponding to the sequence identified in (A).

phosphorylated proteins, for example, GLUD1, PKC $\delta$ , MFN1, COQ8, and MAPK12 (see SI Table 4). Some new phosphorylation sites in previously reported phosphoproteins were discovered for the first time in our study. For instance, the two phosphorylation sites T88 and S94 in rat TOMM70a (Q75Q39) were already present in the UniProtKB Protein knowledgebase and two new phosphorylation sites, S104 and S111, were discovered in our study. It is noteworthy that 12 phosphorylated tyrosine sites were found in our study using a high-throughput shotgun method, more than those previously detected in other studies using shotgun methods.<sup>25,26</sup> These tyrosine phosphorylation sites suggest that tyrosine kinases present within the mitochondria, at least in pancreatic  $\beta$  cells.

**3.5. Analysis of Mitochondrial Signaling Networks.** Since the first phosphorylated protein, PDH, was reported in the late 1960s, dozens of phosphorylated proteins and a few protein kinases have been reported to be present in the mitochondria of different tissues.<sup>19,22</sup> The presence of these kinases or kinase-associated proteins suggest that protein phosphorylation is an important mode of signal pathway regulation within the mitochondria. In this study, many of the mitochondrial phosphoproteins and protein kinases identified play important roles in mitochondria. PDHA, well-known as the rate-limiting en-

zyme of the TCA cycle and for being inhibited by phosphorylation, was found to be phosphorylated at several sites. The 18-kDa protein of oxidative phosphorylation complex 1 has been shown to increase ATP molecule production. GLUD1 is subject to allosteric regulation by ADP, ATP, and GTP. Here, GLUD1 was found to be phosphorylated at S128. We hypothesize that the function of this protein is regulated by both allosteric effects and phosphorylation. Other mitochondrial proteins involved in ATP production which were shown to be phosphorylated include CYB5R3, BCKDHA, ACOX3, and LC-MT2. In addition, VDAC1, VDAC2, ATP2A2, and ATP2A3 may be pivotal channels for mitochondrial calcium influx, and phosphorylation of calcium channels would affect mitochondrial calcium influx. Increasing cytosolic calcium is a prerequisite for GSIS. Following a spike in cytosol calcium, mitochondrial calcium also increases very rapidly, increasing the efficiency of OXPHOS and further enhancing ATP production. We speculate, therefore, that  $\beta$  cells may adjust mitochondrial calcium influx by phosphorylating the above mitochondrial channels, and further regulate the mitochondrial activity to meet the needs of GSIS. In this work, we also discovered that some mitochondrial kinases and kinase-associated proteins, such as PKC $\delta$ , MAPK12, and AKAP1, are phosphorylated. On

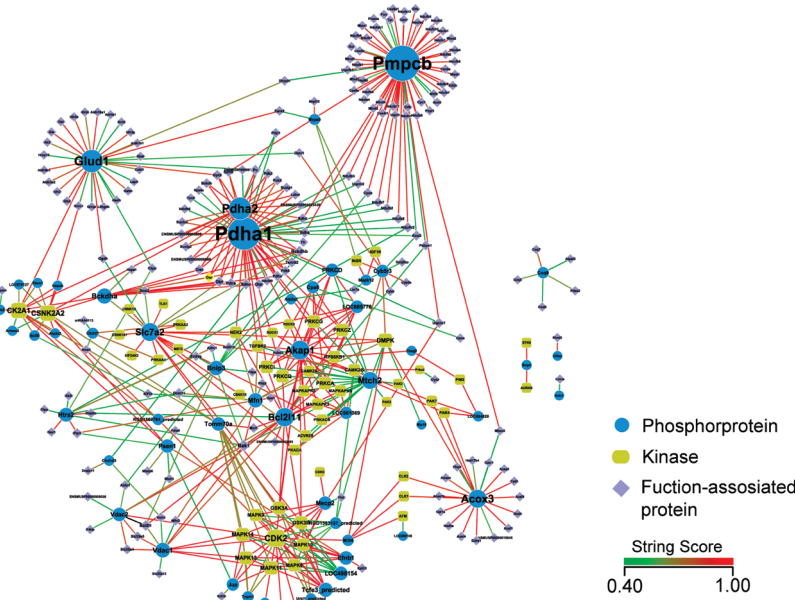


**Figure 4.** The interaction network of identified mitochondrial phosphoproteins, their interacting proteins and upstream kinases. The interaction network was presented using Cytoscape. Blue circles, yellow-green round rectangles, and purple diamonds represent mitochondrial phosphoproteins, their kinases, and the functional interaction proteins of the mitochondrial phosphoproteins, respectively.

the basis of the above analysis, we hypothesized that mitochondrial function is modulated not only by the intermediates of nutrient metabolism, but also by specific signaling from outside of the mitochondria when pancreatic  $\beta$  cells sense glucose fluctuation.

Since there are many phosphoproteins in mitochondria, we wondered which kinases act on these phosphoproteins and what are their upstream signaling pathways? To obtain a systematic overview of the effects of phosphorylation signaling on mitochondrial function and the upstream signaling pathways of the mitochondrial phosphoproteins identified, the interaction networks of mitochondrial proteins phosphorylations were constructed by analyzing the upstream kinases and the neighboring functional interaction proteins of mitochondrial phosphoproteins. Of the 84 mitochondrial phosphoproteins identified, 55 proteins extracted 52 kinases from the human database. A total of 245 kinase and substrate interactions were retrieved by submitting sequences and corresponding phosphorylation sites of all the phosphoproteins to the online-software NetworkKIN-2.0 that offers insight into phosphorylation-modulated interaction networks based on the latest human phosphoproteome from the Phospho.ELM (<http://phospho.elm.eu.org/>) and PhosphoSite (<http://www.phosphosite.org/>) databases (Figure 4).<sup>51</sup> According to this classification, these kinases were mainly grouped into PKC, CK2, p38, JNK, CDK2\_CDK3, GSK3, MAPK, and DMPK groups (Figure 5). The kinase–substrate network of mitochondrial phosphoproteins was then combined with the functional interaction proteins of the mitochondrial phosphoproteins. The combined interaction network was finally integrated using Cytoscape as shown in Figure 4.

As shown in Figure 6, many mitochondrial phosphoproteins plus their interacting proteins formed various functional clusters that were cross-linked to different kinase groups (Figure 6). Thus, we can deduce that these kinases regulate the activation of mitochondrial phosphoproteins, and might further influence the function of the proteins which interact with

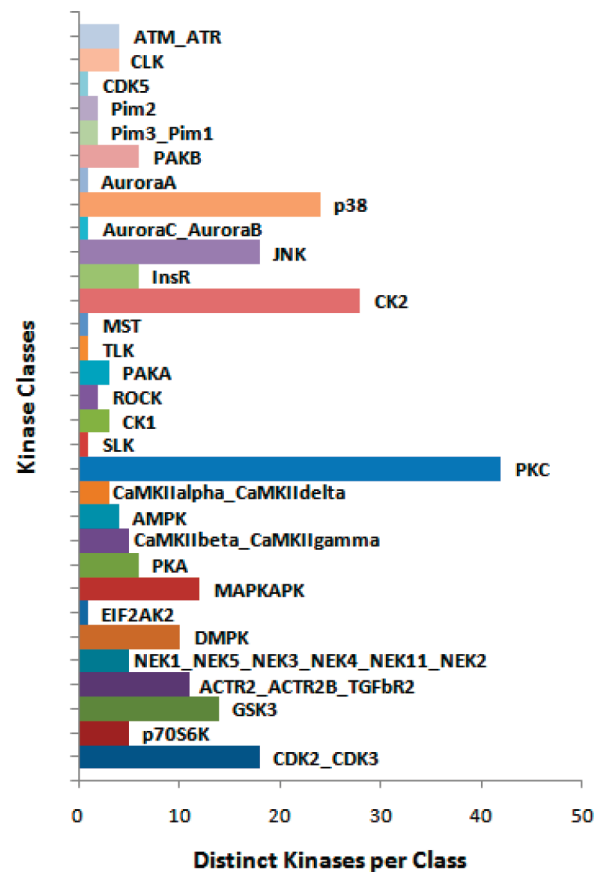


**Figure 5.** Subfamily distribution of protein kinases as predicted by NetworKIN-2.0. The sequences and corresponding phosphorylation sites of all phosphoproteins were submitted to the online-software NetworKIN-2.0 against the latest human phosphoproteome from the Phospho.ELM (<http://phospho.elm.eu.org/>) and PhosphoSite (<http://www.phosphosite.org/>) databases.

mitochondrial phosphoproteins. If these phosphoproteins and their interacting proteins are divided into different biofunc-

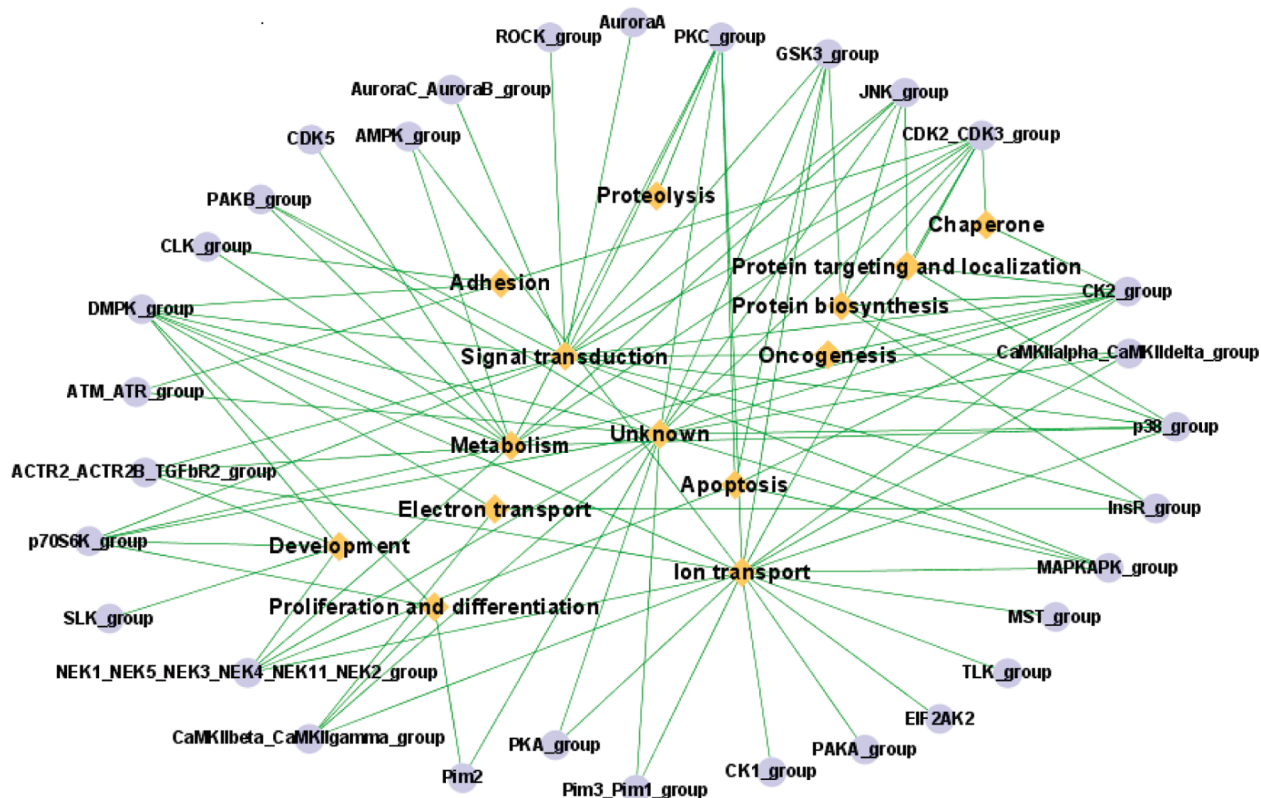


**Figure 6.** Possible effects of different protein kinase groups on mitochondrial function using Cytoscape. Orange diamonds represent different mitochondrial functions, and Cambridge-blue circles represent the classes of mitochondrial kinases.

tional groups based on functional annotation and classification, it can be seen that mitochondrial functions can be regulated by different groups of protein phosphorylation/dephosphorylation (Figure 6). These reversible phosphorylation events possibly control metabolism, electron transport, signal transduction, ion transport, apoptosis, protein targeting and localization, immunity and defense, adhesion, proliferation and differentiation, structure and mobility, development and oncogenesis (Figure 6). Several kinase subgroups, such as PKC and CK2, are known to regulate the OXPHOS system. The presence of many nutrient-activated signaling molecules, such as PKA, PKC, MAPK, and CaMK II, has been detected in the  $\beta$  cell cytosol.<sup>29,58–60</sup> Here we also detected these classes of cytosol protein kinases in the mitochondria. Although integrative pathways connecting cytosol protein kinases and mitochondrial protein kinases remain obscure, we believe that some close linkages exist between them to integrate these signaling pathways together for the maintenance of normal insulin secretion. From this point of view, these nutrients may control insulin secretion not only via producing mitochondria-derived metabolic intermediates, but also by activating cytosol signaling pathways in pancreatic  $\beta$  cells.

**3.6. Implications.** Glucose-stimulated insulin secretion is the key function of  $\beta$  cells and is regulated by mitochondrial-derived metabolites or intermediates in response to blood glucose fluctuation. Results of mitochondrial protein profiling of rat INS-1 pancreatic  $\beta$  cells reported here provide more information about the roles of mitochondria in  $\beta$  cells. In this study, we have discovered many phosphoproteins and their possible kinases, and have shown that some of these phosphoproteins are likely to regulate the production of these mitochondrial metabolites. So, we propose that mitochondrial

function is modulated not only by intermediates of nutrient metabolism, but also by specific phosphorylation signaling from outside of the mitochondria when pancreatic  $\beta$  cells sense nutrient fluctuation. Comparing mitochondrial protein kinases predicted in this study with cytosol nutrient-activated protein kinases previously reported to be present in  $\beta$  cells, it can be seen that there are close links between mitochondrial and cytosol kinases, thus, integrating cytosol signals and mitochondrial signals and maintaining nutrient-activated insulin secretion. We speculate that GSIS is controlled by the intermediates of different kinds of nutrients in mitochondria, and nutrient-activated protein kinase signaling in the cytoplasm.

We present an integrative strategy for analyzing mitochondrial functions including mitochondrial composition and mitochondrial signaling pathways. Integrating the information obtained here on mitochondrial phosphoproteins, with their predicted interacting proteins and upstream kinases, we have produced an overview of how elaborate and reversible phosphorylation reactions regulate mitochondrial function and how intracellular signaling networks regulate the signaling pathways within the mitochondria. Although our findings provide useful information about signaling pathways, they also raise some questions. First, how many signaling pathways are involved in the regulation of mitochondrial function and how do they regulate mitochondrial function? Second, are these proteins imported into the mitochondria in their phosphorylated or unphosphorylated forms?

In summary, mitochondria are so dynamic that it is quite challenging to trace the protein components of mitochondria under different conditions. Our results cannot, therefore, represent the entire contents of mitochondria, and some results, such as new mitochondrial proteins, newly discovered

phosphoproteins, and phosphorylated sites, may need to be verified and updated frequently. However, by dissecting the protein and phosphoprotein composition of  $\beta$  cell mitochondria, this work will lead to greater understanding of mitochondrial function, the effects of mitochondria on the regulation of insulin secretion, and mitochondrial protein changes in diabetes.

**3.7. Abbreviations:** MS, mass spectrometry; GSIS, glucose-stimulated insulin secretion; OXPHOS, oxidative phosphorylation; 2-DE, two-dimensional electrophoresis; MALDI, matrix-assisted laser desorption/ionization; IMAC, immobilized metal ion affinity chromatography; DTT, dithiothreitol; TFA, trifluoroacetic acid; ACN, acetonitrile; PBS, phosphate buffered saline; TEM, transmission electron microscope; TiO<sub>2</sub>, titanium; LTQ, linear trap quadrupole; SCX, strong cation exchange; TPP, Trans-Proteomic Pipeline; GO, gene ontology; KEGG, Kyoto Encyclopedia of Genes and Genomes; PM, plasma membrane; TL, total cell lysis; ER, endoplasmic reticulum; MW, molecular weight; GRAVY, grand average hydropathicity; CAI, Codon Adaptation Index; TCA cycle, tricarboxylic acid cycle; Mud-PIT, multidimensional protein identification technology; PDHA1, pyruvate dehydrogenase E1 alpha 1; TOMM70a, translocase of outer mitochondrial membrane 70 homologue A; GLUD1, glutamate dehydrogenase 1; CYB5R3, cytochrome b5 reductase 3; CaMK II, Ca<sup>2+</sup>/calmodulin-dependent protein kinase IIo; AKAP1, A-kinase anchor protein 1.

**Acknowledgment.** This research was supported by the National Basic Research Program of China (973) (grant no. 2010CB833703, 2010CB833701, 2004CB720004,) and the National Natural Science Foundation of China (grant no. 90919047, 30570466). The authors are indebted to Dr. Joy Fleming for revising and editing the manuscript with valuable suggestions. The authors have declared no conflict of interest.

**Supporting Information Available:** A complete list of all the proteins (SI Table 1), annotated mitochondrial proteins (SI Table 2) and mitochondrial proteins retrieved from KEGG (SI Table 3). A list of the mitochondrial phosphopeptides found in this study (SI Table 4). An expanded discussion on the functional analysis of all the protein groups in the INS-1  $\beta$  cell (SI Data 1). The spectra of all the identified phosphopeptides (SI Data 2). Verification of phosphopeptides identified (SI Data 3). A TEM image of isolated mitochondria (SI Figure 1). Respiration rates of isolated mitochondria (SI Figure 2). Physicochemical characteristics of mitochondrial proteins in INS-1  $\beta$  cells (SI Figure 3). Interactions of mitochondrial proteins (SI Figure 4). Components of the TCA cycle identified by KEGG pathway analysis (SI Figure 5). Components of OXPHOS identified by KEGG pathway analysis (SI Figure 6). This material is available free of charge via the Internet at <http://pubs.acs.org>.

## References

- (1) Reichert, A. S.; Neupert, W. Mitochondriomics or what makes us breathe. *Trends Genet.* **2004**, *20* (11), 555–62.
- (2) Lopez, M. F.; Melov, S. Applied proteomics: mitochondrial proteins and effect on function. *Circ. Res.* **2002**, *90* (4), 380–9.
- (3) Jensen, R. E.; Dunn, C. D.; Youngman, M. J.; Sesaki, H. Mitochondrial building blocks. *Trends Cell Biol.* **2004**, *14* (5), 215–8.
- (4) Au, C. E.; Bell, A. W.; Gilchrist, A.; Hiding, J.; Nilsson, T.; Bergeron, J. J. Organellar proteomics to create the cell map. *Curr. Opin. Cell Biol.* **2007**, *19* (4), 376–85.
- (5) Da Cruz, S.; Parone, P. A.; Martinou, J. C. Building the mitochondrial proteome. *Expert Rev. Proteomics* **2005**, *2* (4), 541–51.
- (6) Rabilloud, T.; Kieffer, S.; Procaccio, V.; Louwagie, M.; Courchesne, P. L.; Patterson, S. D.; Martinez, P.; Garin, J.; Lunardi, J. Two-dimensional electrophoresis of human placental mitochondria and protein identification by mass spectrometry: toward a human mitochondrial proteome. *Electrophoresis* **1998**, *19* (6), 1006–14.
- (7) Pfleider, D.; Le Caer, J. P.; Lemaire, C.; Bernard, B. A.; Dujardin, G.; Rossier, J. Systematic identification of mitochondrial proteins by LC-MS/MS. *Anal. Chem.* **2002**, *74* (10), 2400–6.
- (8) Sickmann, A.; Reinders, J.; Wagner, Y.; Joppich, C.; Zahedi, R.; Meyer, H. E.; Schonfisch, B.; Perschil, I.; Chacinska, A.; Guiard, B.; Rehling, P.; Pfanner, N.; Meisinger, C. The proteome of *Saccharomyces cerevisiae* mitochondria. *Proc. Natl. Acad. Sci. U.S.A.* **2003**, *100* (23), 13207–12.
- (9) Prokisch, H.; Scharfe, C.; Camp, D. G., 2nd; Xiao, W.; David, L.; Andreoli, C.; Monroe, M. E.; Moore, R. J.; Gritsenko, M. A.; Kozany, C.; Hixson, K. K.; Mottaz, H. M.; Zischka, H.; Ueffing, M.; Herman, Z. S.; Davis, R. W.; Meitinger, T.; Oefner, P. J.; Smith, R. D.; Steinmetz, L. M. Integrative analysis of the mitochondrial proteome in yeast. *PLoS Biol.* **2004**, *2* (6), e160.
- (10) Taylor, S. W.; Fahy, E.; Zhang, B.; Glenn, G. M.; Warnock, D. E.; Wiley, S.; Murphy, A. N.; Gaucher, S. P.; Capaldi, R. A.; Gibson, B. W.; Ghosh, S. S. Characterization of the human heart mitochondrial proteome. *Nat. Biotechnol.* **2003**, *21* (3), 281–6.
- (11) Gaucher, S. P.; Taylor, S. W.; Fahy, E.; Zhang, B.; Warnock, D. E.; Ghosh, S. S.; Gibson, B. W. Expanded coverage of the human heart mitochondrial proteome using multidimensional liquid chromatography coupled with tandem mass spectrometry. *J. Proteome Res.* **2004**, *3* (3), 495–505.
- (12) Mootha, V. K.; Bunkenborg, J.; Olsen, J. V.; Hjerrild, M.; Wisniewski, J. R.; Stahl, E.; Bolouri, M. S.; Ray, H. N.; Sihag, S.; Kamal, M.; Patterson, N.; Lander, E. S.; Mann, M. Integrated analysis of protein composition, tissue diversity, and gene regulation in mouse mitochondria. *Cell* **2003**, *115* (5), 629–40.
- (13) Zhang, J.; Li, X.; Mueller, M.; Wang, Y.; Zong, C.; Deng, N.; Vondriska, T. M.; Liem, D. A.; Yang, J. I.; Korge, P.; Honda, H.; Weiss, J. N.; Apweiler, R.; Ping, P. Systematic characterization of the murine mitochondrial proteome using functionally validated cardiac mitochondria. *Proteomics* **2008**, *8* (8), 1564–75.
- (14) Forner, F.; Foster, L. J.; Campanaro, S.; Valle, G.; Mann, M. Quantitative proteomic comparison of rat mitochondria from muscle, heart, and liver. *Mol. Cell. Proteomics* **2006**, *5* (4), 608–19.
- (15) Pagliarini, D. J.; Calvo, S. E.; Chang, B.; Sheth, S. A.; Vafai, S. B.; Ong, S. E.; Walford, G. A.; Sugiana, C.; Boneh, A.; Chen, W. K.; Hill, D. E.; Vidal, M.; Evans, J. G.; Thorburn, D. R.; Carr, S. A.; Mootha, V. K. A mitochondrial protein compendium elucidates complex I disease biology. *Cell* **2008**, *134* (1), 112–23.
- (16) Richly, E.; Chinnery, P. F.; Leister, D. Evolutionary diversification of mitochondrial proteomes: implications for human disease. *Trends Genet.* **2003**, *19* (7), 356–62.
- (17) Meisinger, C.; Sickmann, A.; Pfanner, N. The mitochondrial proteome: from inventory to function. *Cell* **2008**, *134* (1), 22–4.
- (18) Johnson, D. T.; Harris, R. A.; French, S.; Blair, P. V.; You, J.; Bemis, K. G.; Wang, M.; Balaban, R. S. Tissue heterogeneity of the mammalian mitochondrial proteome. *Am. J. Physiol.: Cell Physiol.* **2007**, *292* (2), C689–97.
- (19) Thomson, M. Evidence of undiscovered cell regulatory mechanisms: phosphoproteins and protein kinases in mitochondria. *Cell. Mol. Life Sci.* **2002**, *59* (2), 213–9.
- (20) Goldenthal, M. J.; Marin-Garcia, J. Mitochondrial signaling pathways: a receiver/integrator organelle. *Mol. Cell. Biochem.* **2004**, *262* (1–2), 1–16.
- (21) Salvi, M.; Brunati, A. M.; Toninello, A. Tyrosine phosphorylation in mitochondria: a new frontier in mitochondrial signaling. *Free Radical Biol. Med.* **2005**, *38* (10), 1267–77.
- (22) Pagliarini, D. J.; Dixon, J. E. Mitochondrial modulation: reversible phosphorylation takes center stage. *Trends Biochem. Sci.* **2006**, *31* (1), 26–34.
- (23) Schulenberg, B.; Aggeler, R.; Beechem, J. M.; Capaldi, R. A.; Patton, W. F. Analysis of steady-state protein phosphorylation in mitochondria using a novel fluorescent phosphosensor dye. *J. Biol. Chem.* **2003**, *278* (29), 27251–5.
- (24) Hopper, R. K.; Carroll, S.; Aponte, A. M.; Johnson, D. T.; French, S.; Shen, R. F.; Witzmann, F. A.; Harris, R. A.; Balaban, R. S. Mitochondrial matrix phosphoproteome: effect of extra mitochondrial calcium. *Biochemistry* **2006**, *45* (8), 2524–36.
- (25) Lee, J.; Xu, Y.; Chen, Y.; Sprung, R.; Kim, S. C.; Xie, S.; Zhao, Y. Mitochondrial phosphoproteome revealed by an improved IMAC method and MS/MS/MS. *Mol. Cell. Proteomics* **2007**, *64*, 669–76.
- (26) Reinders, J.; Wagner, K.; Zahedi, R. P.; Stojanovski, D.; Eyrich, B.; van der Laan, M.; Rehling, P.; Sickmann, A.; Pfanner, N.; Meisinger, C. Profiling phosphoproteins of yeast mitochondria reveals a role of phosphorylation in assembly of the ATP synthase. *Mol. Cell. Proteomics* **2007**, *6* (11), 1896–906.

- (27) Lewandrowski, U.; Sickmann, A.; Cesaro, L.; Brunati, A. M.; Toninello, A.; Salvi, M. Identification of new tyrosine phosphorylated proteins in rat brain mitochondria. *FEBS Lett.* **2008**, *582* (7), 1104–10.
- (28) Feng, J.; Zhu, M.; Schaub, M. C.; Gehrig, P.; Roschitzki, B.; Lucchinetti, E.; Zaugg, M. Phosphoproteome analysis of isoflurane-protected heart mitochondria: phosphorylation of adenine nucleotide translocator-1 on Tyr194 regulates mitochondrial function. *Cardiovasc. Res.* **2008**, *80* (1), 20–9.
- (29) Eliasson, L.; Abdulkader, F.; Braun, M.; Galvanovskis, J.; Hoppa, M. B.; Rorsman, P. Novel aspects of the molecular mechanisms controlling insulin secretion. *J. Physiol.* **2008**, *586* (14), 3313–24.
- (30) Maechler, P.; Wollheim, C. B. Mitochondrial signals in glucose-stimulated insulin secretion in the beta cell. *J. Physiol.* **2000**, *529* (Pt 1), 49–56.
- (31) Maechler, P.; Wollheim, C. B. Mitochondrial function in normal and diabetic beta-cells. *Nature* **2001**, *414* (6865), 807–12.
- (32) Maechler, P.; Carobbio, S.; Rubi, B. In beta-cells, mitochondria integrate and generate metabolic signals controlling insulin secretion. *Int. J. Biochem. Cell Biol.* **2006**, *38* (5–6), 696–709.
- (33) Maechler, P.; de Andrade, P. B. Mitochondrial damages and the regulation of insulin secretion. *Biochem. Soc. Trans.* **2006**, *34* (Pt 5), 824–7.
- (34) Newsholme, P.; Bender, K.; Kiely, A.; Brennan, L. Amino acid metabolism, insulin secretion and diabetes. *Biochem. Soc. Trans.* **2007**, *35* (Pt 5), 1180–6.
- (35) Mulder, H.; Ling, C. Mitochondrial dysfunction in pancreatic beta-cells in Type 2 diabetes. *Mol. Cell. Endocrinol.* **2009**, *297* (1–2), 34–40.
- (36) Okado-Matsumoto, A.; Fridovich, I. Subcellular distribution of superoxide dismutases (SOD) in rat liver: Cu, Zn-SOD in mitochondria. *J. Biol. Chem.* **2001**, *276* (42), 38388–93.
- (37) Wu, J.; Shakey, Q.; Liu, W.; Schuller, A.; Follettie, M. T. Global profiling of phosphopeptides by titania affinity enrichment. *J. Proteome Res.* **2007**, *6* (12), 4684–9.
- (38) Romijn, E. P.; Yates, J. R. 3rd. Analysis of organelles by on-line two-dimensional liquid chromatography-tandem mass spectrometry. *Methods Mol. Biol.* **2008**, *432*, 1–16.
- (39) Keller, A.; Nesvizhskii, A. I.; Kolker, E.; Aebersold, R. Empirical statistical model to estimate the accuracy of peptide identifications made by MS/MS and database search. *Anal. Chem.* **2002**, *74* (20), 5383–92.
- (40) Nesvizhskii, A. I.; Keller, A.; Kolker, E.; Aebersold, R. A statistical model for identifying proteins by tandem mass spectrometry. *Anal. Chem.* **2003**, *75* (17), 4646–58.
- (41) Cociorva, D.; Tabb, D. L.; Yates, J. R., III. Validation of tandem mass spectrometry database search results using DTASelect. In *Current Protocols in Bioinformatics*; Baxevanis, A. D.; Yates, J. R., III, Eds.; Wiley & Sons, Inc.: NJ, 2007.
- (42) Beausoleil, S. A.; Villen, J.; Gerber, S. A.; Rush, J.; Gygi, S. P. A probability-based approach for high-throughput protein phosphorylation analysis and site localization. *Nat. Biotechnol.* **2006**, *24* (10), 1285–92.
- (43) Emanuelsson, O.; Nielsen, H.; Brunak, S.; von Heijne, G. Predicting subcellular localization of proteins based on their N-terminal amino acid sequence. *J. Mol. Biol.* **2000**, *300* (4), 1005–16.
- (44) Claros, M. G.; Vincens, P. Computational method to predict mitochondrial imported proteins and their targeting sequences. *Eur. J. Biochem.* **1996**, *241* (3), 779–86.
- (45) Small, I.; Peeters, N.; Legeai, F.; Lurin, C. Predotar: A tool for rapidly screening proteomes for N-terminal targeting sequences. *Proteomics* **2004**, *4* (6), 1581–90.
- (46) Hua, S.; Sun, Z. Support vector machine approach for protein subcellular localization prediction. *Bioinformatics* **2001**, *17* (8), 721–8.
- (47) Wilkins, M. R.; Gasteiger, E.; Bairoch, A.; Sanchez, J. C.; Williams, K. L.; Appel, R. D.; Hochstrasser, D. F. Protein identification and analysis tools in the ExPASy server. *Methods Mol. Biol.* **1999**, *112*, 531–52.
- (48) Thomas, P. D.; Campbell, M. J.; Kejariwal, A.; Mi, H.; Karlak, B.; Daverman, R.; Diemer, K.; Muruganujan, A.; Narechania, A. PANTHER: a library of protein families and subfamilies indexed by function. *Genome Res.* **2003**, *13* (9), 2129–41.
- (49) Thomas, P. D.; Kejariwal, A.; Campbell, M. J.; Mi, H.; Diemer, K.; Guo, N.; Ladunga, I.; Ulitsky-Lazareva, B.; Muruganujan, A.; Rabkin, S.; Vandergriff, J. A.; Doremieux, O. PANTHER: a browsable database of gene products organized by biological function, using curated protein family and subfamily classification. *Nucleic Acids Res.* **2003**, *31* (1), 334–41.
- (50) Jensen, L. J.; Kuhn, M.; Stark, M.; Chaffron, S.; Creevey, C.; Muller, J.; Doerks, T.; Julien, P.; Roth, A.; Simonovic, M.; Bork, P.; von Mering, C. STRING 8--a global view on proteins and their functional interactions in 630 organisms. *Nucleic Acids Res.* **2009**, *37* (Database issue), D412–6.
- (51) Linding, R.; Jensen, L. J.; Ostheimer, G. J.; van Vugt, M. A.; Jorgensen, C.; Miron, I. M.; Diella, F.; Colwill, K.; Taylor, L.; Elder, K.; Metalnikov, P.; Nguyen, V.; Pascalescu, A.; Jin, J.; Park, J. G.; Samson, L. D.; Woodgett, J. R.; Russell, R. B.; Bork, P.; Yaffe, M. B.; Pawson, T. Systematic discovery of in vivo phosphorylation networks. *Cell* **2007**, *129* (7), 1415–26.
- (52) Shannon, P.; Markiel, A.; Ozier, O.; Baliga, N. S.; Wang, J. T.; Ramage, D.; Amin, N.; Schwikowski, B.; Ideker, T. Cytoscape: a software environment for integrated models of biomolecular interaction networks. *Genome Res.* **2003**, *13* (11), 2498–504.
- (53) Frezza, C.; Cipolat, S.; Scorrano, L. Organelle isolation: functional mitochondria from mouse liver, muscle and cultured fibroblasts. *Nat. Protoc.* **2007**, *2* (2), 287–95.
- (54) Chen, E. I.; Cociorva, D.; Norris, J. L.; Yates, J. R., III. Optimization of mass spectrometry-compatible surfactants for shotgun proteomics. *J. Proteome Res.* **2007**, *6* (7), 2529–38.
- (55) Okuda, S.; Yamada, T.; Hamajima, M.; Itoh, M.; Katayama, T.; Bork, P.; Goto, S.; Kanehisa, M. KEGG Atlas mapping for global analysis of metabolic pathways. *Nucleic Acids Res.* **2008**, *36* (Web Server issue), W423–6.
- (56) Yaney, G. C.; Corkey, B. E. Fatty acid metabolism and insulin secretion in pancreatic beta cells. *Diabetologia* **2003**, *46* (10), 1297–312.
- (57) Herrero, L.; Rubi, B.; Sebastian, D.; Serra, D.; Asins, G.; Maechler, P.; Prentki, M.; Hegardt, F. G. Alteration of the malonyl-CoA/carnitine palmitoyltransferase I interaction in the beta-cell impairs glucose-induced insulin secretion. *Diabetes* **2005**, *54* (2), 462–71.
- (58) Jones, P. M.; Persaud, S. J. Protein kinases, protein phosphorylation, and the regulation of insulin secretion from pancreatic beta-cells. *Endocr. Rev.* **1998**, *19* (4), 429–61.
- (59) Sjoholm, A.; Lehtihet, M.; Efsanov, A. M.; Zaitsev, S. V.; Berggren, P. O.; Honkanen, R. E. Glucose metabolites inhibit protein phosphatases and directly promote insulin exocytosis in pancreatic beta-cells. *Endocrinology* **2002**, *143* (12), 4592–8.
- (60) Berggren, P. O.; Leibiger, I. B. Novel aspects on signal-transduction in the pancreatic beta-cell. *Nutr. Metab. Cardiovasc. Dis.* **2006**, *16* (Suppl. 1), S7–10.

PR100139Z